

Geochemistry of coarse quartz sinter overlying an Early Cretaceous Serra Geral quartz andesite flow, Fronteira Oeste Rift, Rio Grande do Sul, Brazil

Léo Afraneo Hartmann^{1*} , Melissa Johner¹ , Gláucia Nascimento Queiroga² 

Abstract

Sinter overlying the first quartz andesite flow at the base of the Serra Geral Group is a surface manifestation of intense hydrothermal processes operating in the Paraná Basin during the Early Cretaceous. The coarse quartz sinter from western Rio Grande do Sul state was studied in satellite images, field surveying, optical petrography, scanning electron microscopy, and electron probe microanalyses, including backscattered electron images and chemical analyses of rocks. Quartz forms large crystals (10 cm) because it was either deposited in a dilute aqueous solution or recrystallized from fine-grained sinter. Well-crystallized chamosite — an iron aluminosilicate (Fe-chlorite) — occurs in quartz crystals, partly associated with fractures. The composition of chamosite is akin to that in ore deposit associations. Noble metals in two sinter samples are present in concentrations of 0.1 ppm Ag and 15 ppb Au. The contents of Ba, Bi, Cu, Mo, S, and W are low but are significant. The present description of sinter quartz signals the presence of a major paleo-hot spring field in the Fronteira Oeste Rift, Rio Grande do Sul, Brazil, that merits further study to fully characterize the extent and metallogenetic endowment (Au-Ag-Cu) of the epithermal province.

KEYWORDS: coarse quartz sinter; chamosite; epithermal Au-Ag-Cu; Serra Geral Group; Fronteira Oeste Rift; geochemistry.

INTRODUCTION

The Paraná Volcanic Province (1 million km²) has an extensive and thick (up to 1,700 m) tholeiitic volcanic sequence of basalt (97.5%) and rhyodacite (2.5%) flows encased in the Serra Geral Group. Basalt, quartz andesite, and rhyodacite host the largest world deposits of amethyst and agate geodes, both in the first lava flows and in several stratigraphic positions up to 1,000 m above the first flow. Long considered magmatic in origin by degassing of the lava, the natural history of the geodes started to be elucidated by temperature determination of amethyst crystallization at 50°C (e.g., Juchem 1999). A significant contribution by Gilg *et al.* (2003) clarified the origin of the mineralizing fluids from the Guarani Aquifer. Extensive alteration of the mineralized basalt by low-temperature minerals was established by Gomes (1996). The origin of the geodic cavity was described by Duarte *et al.* (2009) as low-temperature ballooning of altered basalt. Lowering the temperature resulted in the partial filling of the geode with valuable minerals. The hydrothermal, epigenetic origin of the geodes was thus established. A pervasive hydrothermal event was recognized in the

Serra Geral Group, forming low-temperature minerals (zeolites, clays, and native copper) in the amygdaloides and fractures during the first hydrothermal event (H1). Hot water continued to be pressurized below the sealed basalt, leading to the explosive injection and effusion (H2) of fluidized sand, which originated in the underlying Guarani Aquifer. A description of the aquifer is in Hirata and Foster (2021). Newly sealed basalt was affected by hot water percolation (H3), leading to the opening and filling of geodes.

The hydrothermal partial alteration of basalt in most flows could evolve in some places to the emission of hot vapor at the paleosurface, forming hot springs in the Early Cretaceous (Hartmann *et al.* 2021, 2022a). Volcanism occurred near 134.5 Ma (e.g., Hartmann *et al.* 2019, Gomes and Vasconcelos 2021). Thick soil and forest cover (remnants of the Atlantic Forest) and the focus by researchers on volcanic aspects of the group impeded the finding of paleohot springs. Hydrothermal processes that altered the basaltic lavas in the Cretaceous started to be recognized from the work of Duarte *et al.* (2009) and Hartmann *et al.* (2012). Further field work by these authors focused on identifying the paleohot springs. A change in paradigm was required to make possible the discovery of the surficial effusion of hot water and related deposits. The distal imprint of paleodune shape formed rings and arcs in the upper amygdaloidal crust of the Catalán Flow (Hartmann *et al.* 2021). Additional studies are required to fully characterize the sinter, because of the scientific and potential economic importance of the previous finding by Hartmann *et al.* (2022a). Silicification, fracturing, and steam venting in paleodunes were evaluated by Hartmann *et al.* (2022b) and in volcanic rocks by Hartmann *et al.* (2021).

¹Instituto de Geociências, Universidade Federal do Rio Grande do Sul – Porto Alegre (RS), Brazil. E-mails: leo.hartmann@ufrgs.br, melissajohner@hotmail.com

²Departamento de Geologia, Escola de Minas, Universidade Federal de Ouro Preto – Ouro Preto (MG), Brazil. E-mail: glauciaqueiroga@ufop.edu.br

*Corresponding author.



We selected the sinter from the Macacos Locale for a study of this first identification of paleohot spring activity in the Paraná Volcanic Province. We further characterized the sinter with several techniques, following the initial report by Hartmann *et al.* (2022a). We integrated field surveying with petrography, scanning electron microscopy (SEM), energy dispersive spectrometry (EDS) analyses, backscattered electron (BSE) imaging, electron probe microanalyzer (EPMA) imaging, and chemical analyses of quartz and chamosite. Sinter was analyzed for major and trace elements. The sinter has chamosite (Fe-chlorite) with quartz (some gypsum and barite), which is significant for the indication of an epithermal Au-Ag-Cu metallogenetic province. Au and Ag contents are in the low range of mineralized epithermal provinces (e.g., Yellowstone; Churchill *et al.* 2021). The fountain that generated the sinter was active above the first lava flow that covered the active dunes. This is the description of the first window into the surficial hydrothermal processes operative in a large area (> 15,000 km²) of the Serra Geral Group (Fronteira Oeste Rift) during the initial stages of effusion of lavas in the Early Cretaceous.

GEOLOGICAL SETTING

The South American Serra Geral Group occurs mostly in Brazil, and also in Uruguay, Argentina, and Paraguay (Figs. 1A, 1B), with a fragment (8%) drifted to southwestern Africa during rupturing of Gondwana (e.g., Hartmann *et al.* 2010, 2019). Volcanic rocks are near the top of the Paraná Basin (Zalán *et al.* 1991), only covered by the Bauru Group sedimentary and volcanic rocks. Sedimentary rocks attained > 200°C in the northeastern part of the basin (Teixeira *et al.* 2018). The large (1 million km²) volcanic group has been described for its volcanic characteristics, with a tendency to attribute to volcanism all features observed in the field. Intercalated sand layers have been systematically attributed to eolian deposition (e.g., Bertolini *et al.* 2020, 2021).

The discovery of injection and effusive structures associated with the sand bodies associated with the lavas (Hartmann *et al.* 2010, Duarte *et al.* 2020) in the Novo Hamburgo Complex (Fig. 2, Table 1) was integrated with the processes that led to the universal presence of injected sand in the amethyst geode deposits. The initial observation of sand in geodes

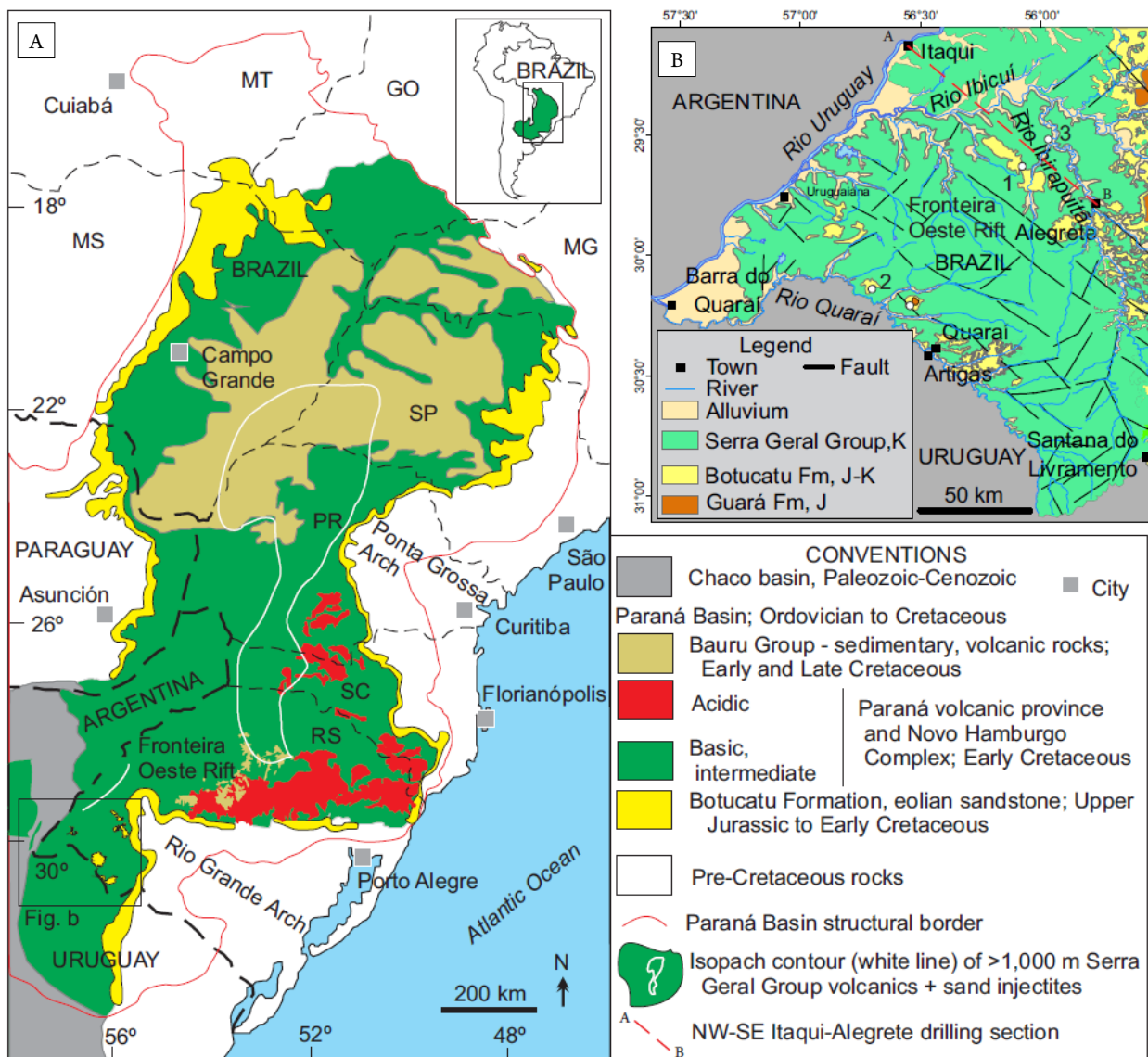


Figure 1. (A) Geological map of the Serra Geral Group, underlying Botucatu Formation and overlying Bauru Group; external limit of Paraná Basin indicated; map from Hartmann and Cerva-Alves (2021). Location of (B) is shown. (B) Geological map of Fronteira Oeste Rift (simplified from Silva *et al.* 2004); 1: Macacos Locale; 2: Santa Helena Paleodune; 3: Camoatim Paleodune.

was made by Bossi and Caggiano (1974) and consolidated with the correct hydrothermal interpretation by Duarte *et al.* (2009). Hot water was perceived as altering the basalt and opening and filling cavities in the cold (50–150°C) rock. In many outcrops, filled fractures point to shallow levels near the surface; many geodes in the mines have escape channels of fluid above their tops. It seemed reasonable that some of

the fractures reached the surface as hot springs and geysers. A specific search was required.

The Fronteira Oeste Rift (Hartmann and Cerva-Alves 2021) has six flat-lying lava flows distributed in layer-cake stratigraphy (Fig. 2). Sand dikes, sills, and extrudites are common in the rift. Rifting postdated the Serra Geral Group by 10–15 Ma in the region. Both exposed paleodune tops and

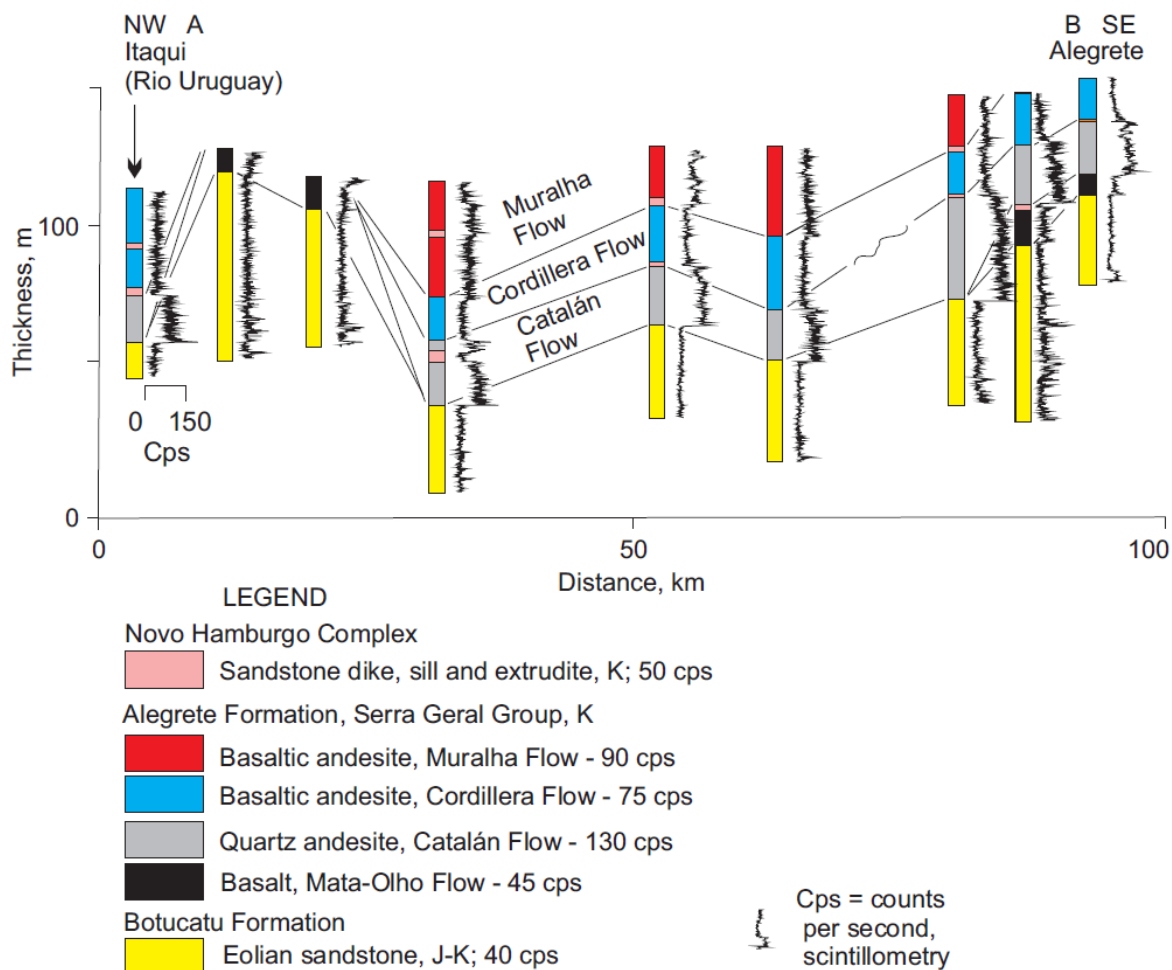


Figure 2. Drilling section between Alegrete and Itaquí; drill hole logs projected orthogonally to section line from up to 10 km on either side.

Table 1. Nomenclature of stratigraphic and other units of the Paraná Basin in the studied Fronteira Oeste region of Brazil in Rio Grande do Sul state.

Units, Age	Description
<i>Stratigraphy</i>	
Novo Hamburgo Complex, 134.5 ± 2 Ma	Sand injectites in the Serra Geral Group — dikes, sills, and extrudites
Serra Geral Group (Paraná Volcanic Province), Early Cretaceous, 134.5 ± 2 Ma	Muralha Flow (basaltic andesite)
	Cordillera Flow (basaltic andesite)
	Catalán Flow (andesite)
	Mata-Olho Flow (basalt)
Botucatu Formation, Late Jurassic-Early Cretaceous, 134.5 ± 2 Ma	Quartz dunes and sand sheets
Guará Formation, Late Jurassic	Fluvial and eolian sandstones
<i>Other units</i>	
Fronteira Oeste Paleohot Spring Field, Early K	Extensive occurrence of thousands of hydrothermal bowls and fumaroles at the top of paleodunes and three first lava flows. One silica sinter occurrence
Inhanduí Paleodune Field, J-Early K	Large (30 × 10 km) dune field aligned NW from Alegrete town, starting near Rio Inhanduí
Guaviju Rings and Arcs Field, Early K	Extensive (150 × 150 km) distribution of erosional remnants of silicified (sand injectites, quartz veins, and amygdale filling) upper amygdaloidal crust of Catalán Flow

overlying volcanic rocks were fractured into rhomboids by forces related to a vertical σ_1 ellipsoid (e.g., Hartmann *et al.* 2021). Hot water reaching the surface was first identified in the presently studied sinter (Figs. 3 and 4) (Hartmann and Cerva-Alves 2021) and then by Hartmann *et al.* (2022) in a 50-cm large hydrothermal bowl at the top of a paleodune from the Botucatu Formation.

METHODOLOGY

Similar methodology was used as described by Hartmann and Cerva-Alves (2021) and Hartmann *et al.* (2022a). Volcanic rock classification follows Santos and Hartmann (2021). Satellite images were interpreted by Hartmann *et al.* (2021) for the local understanding of the distribution of massive core and elliptical crust remnants of the Catalán Flow. Images were from GoogleEarth, which is based on Landsat images. Field work was done in the Macacos Locale to describe and interpret the previously identified coarse quartz sinter, including sample (n = 3) collection. Samples MAC3, MAC4, and MAC6 were studied with the optical microscope and SEM at the Laboratório de Geologia Isotópica, Centro de Estudos em Petrologia e Geoquímica, Instituto de Geociências, Universidade Federal de Rio Grande do Sul. The SEM is a JEOL JSM-6610LV, equipped with a Bruker XFLASH 5030 energy dispersive X-ray spectrometer. Analytical conditions were 20 kV, spot size 60 μm , working distance 0.7 mm, and counting time 30 s for the EDS analyses.

Sample MAC6 was additionally investigated with the SEM and EPMA in a new thin section. Mineral chemistry was acquired with an electron microprobe JEOL JXA-8230 at the Microscopy and Microanalysis Laboratory, Universidade Federal de Ouro Preto. The mineral chemistry was determined on quartz (to confirm identification) and chamosite under conditions of 15 kV accelerating voltage, 20 nA sample current, and 5 μm spot size; ZAF matrix corrections were applied. Counting times on the peaks and background were 10/5 s for all elements. Analytical errors are 0.21–1.43%. Standards used are listed in Cerva-Alves *et al.* (2021). BSE images were made for textural characterization and spot location for chemical analyses. Mineral abbreviations are from Whitney and Evans (2010).

The identification of chamosite was initially made on the webmineral site of the International Mineralogical Association (IMA, 2022). The chemical composition of the mineral determined by EPMA led to its only classification as chamosite. A check on the international literature showed no other mineral with a similar composition.

The calculation of chamosite formula followed standard procedures using the results from the EPMA. We used 28 O and applied the sequence of steps from Appendix 1 in Deer *et al.* (1966). All iron was considered as Fe^{2+} . F was calculated separately from O.

The three whole-rock samples (MAC3, MAC4, and MAC6) were analyzed for major and trace elements at GEOSOL, Belo Horizonte, Brazil. Major oxides were analyzed by XRF79C — fusion with lithium tetraborate, analysis by X-ray fluorescence; trace elements by ICM14B — digestion with aqua regia, analysis by ICP OES/ICP MS. Au was analyzed by FAA313 — fire assay AAS, 30 g; and LOI by PHY01E — loss on ignition by gravimetry at 1,000°C.

RESULTS

Integrated study by Hartmann and Cerva-Alves (2021) and Hartmann *et al.* (2021), and additional geological survey led to description of elliptical, gray rings and arcs overlying the quartz andesite core. In the studied Macacos Locale, green grasslands cover the core rocks because of humid summer.

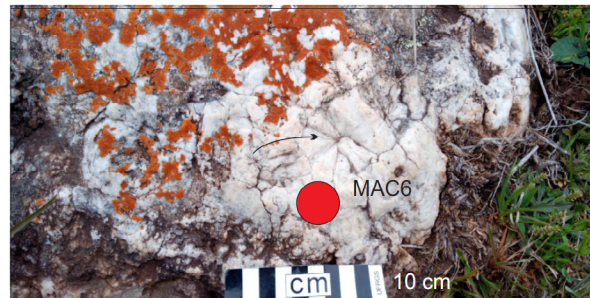


Figure 4. Block of coarse quartz sinter with radiating crystals (indicated by black arrow); quartz partly covered by orange lichen; location of sample MAC6 is shown as red circle. Samples MAC3 and MAC4 were collected within a few meters from this block. Two Catalán quartz andesite samples from the same outcrop were analyzed chemically by Hartmann and Cerva-Alves (2021).

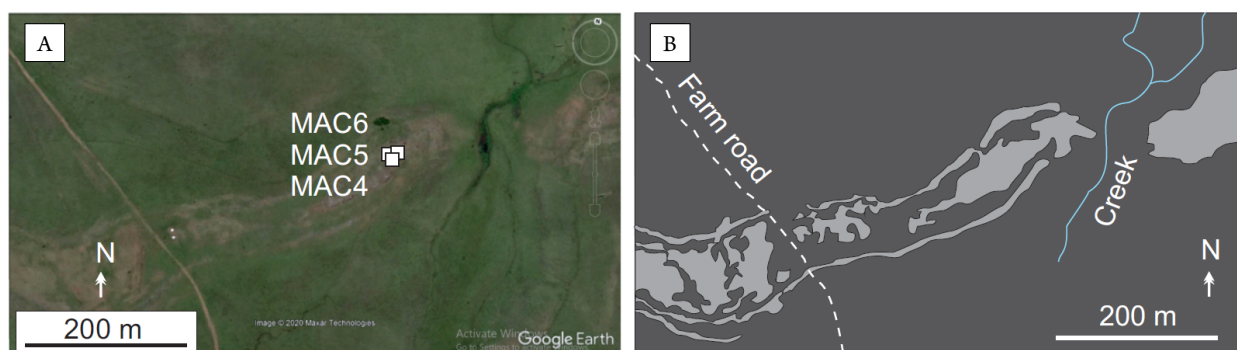


Figure 3. (A) Satellite image of Macacos Locale, showing location of collected sinter samples MAC4, MAC5, and MAC6; gray-colored portions are the silicified upper amygdaloidal crust of the Catalán Flow, which is flat lying (interrupted by creek), two white dots near farm road are animal feeders. (B) Geological map of same area as (A). Brown color corresponds to the massive core of the Catalán Flow, covered with grass and displaying few, small rock blocks. Light gray areas are erosional remnants of the silicified upper amygdaloidal crust of the Catalán Flow.

In cold winter, brown soil is more apparent in the images (Hartmann *et al.* 2021). Paleodunes are not exposed in the studied region; injected, silicified sandstone occurs as blocks (10–50 cm long) included in the upper amygdaloidal portion of the quartz andesite. In places, sandstone dikes evolve into quartz veins along the same fracture.

In the studied Macacos Locale (Figs. 3A, 3B), the exposed geology is dominated by the Catalán Flow. In large extensions, the massive core is exposed below the grasslands, because the upper amygdaloidal crust was eroded. But erosional remnants of the silicified upper amygdaloidal crust are preserved in rings and arches, as described by Hartmann *et al.* (2021). Sinter quartz occurs as 0.5–2.0 m large blocks (Fig. 4) at the top of the amygdaloidal upper crust of the quartz andesite. The white crystals are large (5–10 cm), locally forming radiating bundles. Large quartz crystals contain associated chamosite inclusions (200 μm long) along fractures (Figs. 5A, 5B) (Tables 2 and 3; Fig. 6). The mineral is type I chlorite, trioctahedral, Fe-chlorite in general (Zane and Weiss 1998). EPMA analyses ($n = 15$; not shown) of quartz yield nearly pure SiO_2 .

Whole-rock composition of sample MAC6 (Table 4) displays high CaO (0.36–0.64 wt.%) and S (0.22–0.37 wt.%), with no corresponding minerals identified in the studied thin section. Two sinter samples have near 0.1 ppm Ag and 15 ppb Au. The same two samples that display significant noble metal content also have some trace elements above the detection limit — Ba, Bi, Cu, Mo, S, and W.

DISCUSSION

This study of the first find of sinter blocks overlying a lava flow in the Serra Geral Group points to the presence of a significant paleohot spring field in the southern Paraná Basin. The studies by Hartmann and Cerva-Alves (2021) and Hartmann *et al.* (2021, 2022) indicated intense hydrothermal activity in the Early Cretaceous within the underlying eolian paleodunes of the Botucatu Formation and the first two overlying lava flows — Mata Olho (basalt) and Catalán (quartz andesite) Flows. Scintillometric readings in the field (130 cps) and chemical analyses (Hartmann and Cerva-Alves 2021) of the footwall quartz andesite (e.g., $\text{TiO}_2 = 1.7$ wt.%) are characteristic

properties of the Catalán Flow. Identification of hot spring activity above this quartz andesite opens a large window into processes active in the Paraná Province.

The coarse quartz was formed by one of two possible processes — either direct crystallization from hot water containing

Table 2. Chemical analyses (wt.%) by EPMA of studied chamosite and structural formulae (based on 28 O), sample MAC6.

Spot	1	5	6
SiO_2	32.23	33.89	36.60
TiO_2	0.47	0.64	0.62
Al_2O_3	15.40	15.50	17.44
FeO	36.90	35.64	29.86
MnO	0.07	0.09	0.09
MgO	0.54	0.61	0.68
CaO	0.47	0.56	0.62
Na_2O	0.05	0.05	0.04
K_2O	0.19	0.18	0.26
P_2O_5	0.88	0.70	0.57
F	–	0.02	0.01
Cr_2O_3	0.03	0.01	0.02
Total	87.25	87.90	86.82
Si	7.122	7.277	7.676
$^{\text{IV}}\text{Al}$	0.878	0.723	0.324
$^{\text{VI}}\text{Al}$	3.133	3.199	3.985
Ti	0.078	0.103	0.098
Cr	0.105	0.002	0.004
Fe	6.819	6.399	5.236
Mn	0.013	0.017	0.016
Mg	0.179	0.195	0.212
Ca	0.112	0.129	0.139
Na	0.020	0.021	0.017
K	0.013	0.012	0.017
P	1.032	0.798	0.638
F	0.000	0.012	0.003
Total	18.106	16.875	16.897

Cl, Ba, Sr, and (–): below detection limits.

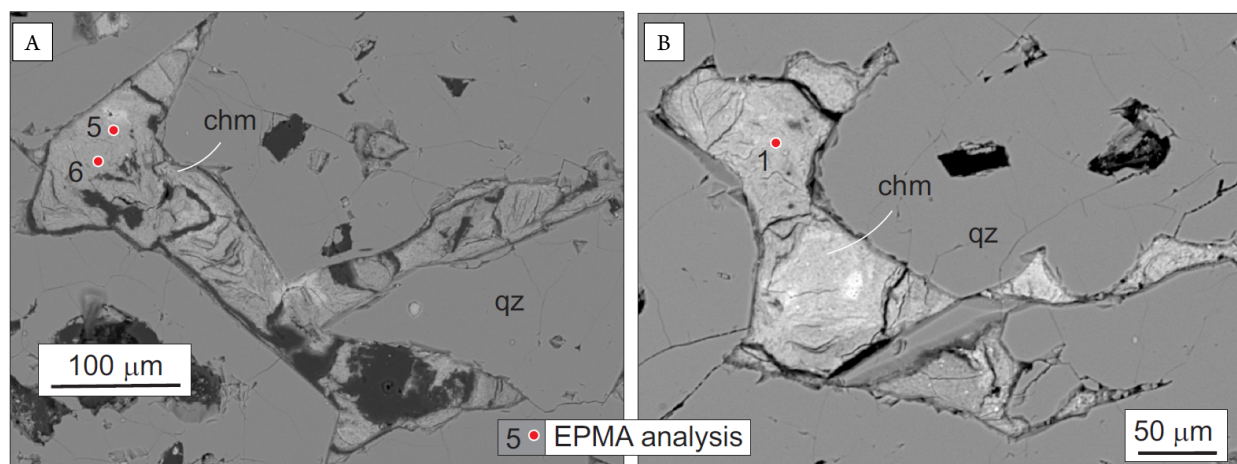
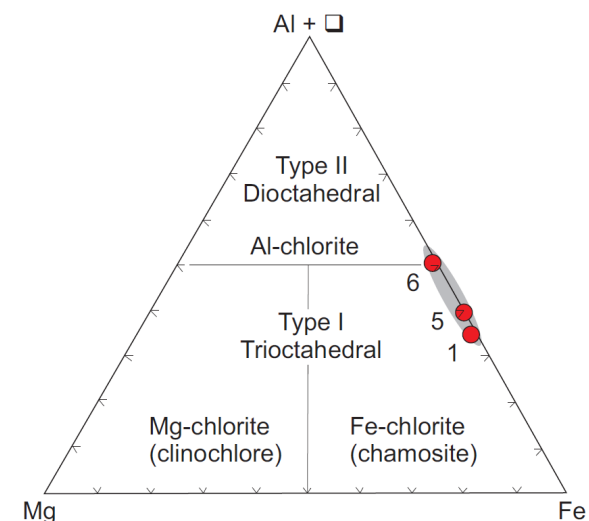


Figure 5. (A and B) BSE images of chamosite crystals contained in coarse quartz and distributed particularly along fractures. EPMA analytical points marked. Dark patches are defects on the thin section.

Table 3. Structural-chemical formulae of analyzed chamosite by EPMA.

Analysis number	Structural formula
1	$^{VI}(Al_{3.13}Na_{0.02}Mg_{0.18}Fe_{6.82}P_{1.03}Ti_{0.08}Ca_{0.11}Cr_{0.01}K_{0.01}Mn_{0.01}\square_{0.60})_{12}^{IV}(Si_{7.12}Al_{0.88})_8(O,OH,F)_{28}$
5	$^{VI}(Al_{3.20}Na_{0.02}Mg_{0.20}Fe_{6.40}P_{0.80}Ti_{0.10}Ca_{0.13}Cr_{0.002}K_{0.01}Mn_{0.02}\square_{1.12})_{12}^{IV}(Si_{7.27}Al_{0.72})_8(O,OH,F)_{28}$
6	$^{VI}(Al_{3.98}Na_{0.02}Mg_{0.21}Fe_{5.24}P_{0.64}Ti_{0.10}Ca_{0.14}Cr_{0.004}K_{0.02}Mn_{0.02}\square_{1.63})_{12}^{IV}(Si_{7.68}Al_{0.32})_8(O,OH,F)_{28}$
General formula	$^{VI}(R_x^{2+}R_y^{3+}\square_{12-x-y})_{12}^{IV}(Si_zR_{8-z}^{3+})_8O,OH_{28}$



Source: Zane and Weiss (1998).

Figure 6. Simplified classification of chlorite from the Macacos sinter. The analyzed chlorite is chamosite.

diluted silicon or recrystallization of fine, opal sinter along time (Jones 2021). A few thousand years seems sufficient for this transformation at 50–150°C.

Opal and chalcedony from surficial sinter are commonly transformed with time (> 50,000 years) into fine and coarse quartz (Marcoux *et al.* 2004). For instance, Holocene sinter from the Yellowstone caldera displays this relationship within a few million years (Kharaka *et al.* 2000, Tan *et al.* 2020). The coarse quartz from the Macacos Locale may correspond to the alteration (diagenesis) of surficial chalcedony from Early Cretaceous sinter.

The blocks bear no resemblance to geodes formed within the lava, which are well-known in the volcanic province (e.g., Duarte *et al.* 2009, Hartmann *et al.* 2012). Chamosite crystallization in fractures of quartz indicates Fe-rich hot water discharge at the paleosurface. Common in sea-floor sedimentary rocks, chamosite was originated from crystallization of terrestrial weathering or volcanic components (Clement *et al.* 2020). Hydrothermal alteration of quartz andesite and remobilization of iron are presently considered for the origin of chamosite in the sinter.

The content of CaO and S in the sinter may correspond to calcite and pyrite present in the sample. The measured Ag and Au in two chemical analyses of sinter suggest an environment prone to noble metal occurrences, because the concentrations are in the lower range of known epithermal deposits. Examples are the Milestone deposit, Idaho deposit (Fenner *et al.* 2022), and deposits in the Yellowstone (Churchill *et al.* 2021). The content of Au (16 and 15 ppb) from the Macacos

Table 4. Whole-rock chemical analyses of studied sinter. Oxides and S in wt.%, trace elements in ppm, Au in ppb.

Sample	MAC3	MAC4	MAC6
SiO ₂	99.0	98.4	97.8
Al ₂ O ₃	0.10	0.13	-
CaO	0.64	0.36	0.61
K ₂ O	0.01	0.01	-
Fe ₂ O ₃	0.20	0.13	0.14
MnO	0.01	-	0.02
LOI	0.84	0.91	0.77
SUM	100.8	99.94	99.34
Ag	-	0.12	0.03
Au	-	16	15
Ba	15	37	42
Bi	-	0.19	0.09
Cd	0.02	-	0.02
Ce	1.38	0.59	2.93
Co	1.8	0.3	2.0
Cr	1	2	3
Cu	1.3	4.4	3.7
Ga	0.2	0.1	0.1
La	0.1	0.2	0.2
Mo	0.20	0.36	0.27
Ni	-	0.7	0.5
Pb	0.7	1.5	0.9
Rb	0.2	0.2	-
S	0.36	0.22	0.37
Sc	0.8	0.7	0.4
Sr	10.5	12.7	14.1
U	0.10	0.25	0.27
V	7	2	5
W	0.2	0.3	0.4
Y	0.10	0.13	0.11
Zn	1	1	2

MgO, Na₂O, P₂O₅, TiO₂, As, B, Be, Cs, Ge, Hf, Hg, In, Li, Lu, Nb, Re, Sb, Se, Sn, Ta, Tb, Te, Th, Yb, Zr, and (-): below detection limits.

sinter is within the range of the old sinter from Yellowstone (2–19 ppb), whereas the content of Ag (16 and 15 ppm) is much higher than Ag in the old sinter (22–44 ppb). The measured contents of Ba, Bi, Cu, Mo, S, and W are an indication of the epithermal environment of sinter deposition.

A test of geological affinity of the chamosite chemistry was made based on the studies by Rivas-Sanchez *et al.* (2006). The contents of cations from the formula unit were plotted (not

shown here) in the following binary and ternary diagrams: $Al \times Fe \times Mg$, $Al/Si \times Mg/Fe$, $(Fe + Mg + Mn) \times Si \times Al$. The compositions of the analyzed chamosite plot inside or close to the field of “ore” in “continental” environments. This affinity reinforces our interpretation of a fertile Fronteira Oeste Rift for epithermal Au-Ag-Cu deposits.

Additional investigations may locate more outcrops of varied sinter rocks and possibly economic concentrations of Au-Ag-Cu. Sinter at the Macacos Locale overlies the second lava flow of the Serra Geral Group, creating a need to study the local and regional geology to fully characterize the paleo-hot spring field and its metallogeny.

CONCLUSION

Our integrated study of a coarse quartz sinter overlying the first lava that covered the Botucatu paleodunes shows the high content of Au and Ag (+Ba, Bi, Cu, Mo, S, and W) in the rock and the presence of accessory chamosite (some gypsum and barite). This first description of sinter above a volcanic flow from the Serra Geral Group opens a wide window into scientific and economic studies of the Fronteira Oeste region

of southernmost Brazil. We thus report the characterization of sinter, which is commonly indicative of the presence of epithermal deposits of Au-Ag-Cu.

ACKNOWLEDGMENTS

We acknowledge the participation in the field by Juliana Pertille da Silva, Sandro Kucera Duarte, Tiara Cerva Alves, Carol M. Custódio, and Vitor Casagrande Dias. We thank the kind hospitality of the landowners. Vitor P. Pereira was most helpful in the calculations regarding chamosite chemical composition and structural formula. Denise Moreira Canarim prepared high-quality thin sections, and Daniel Triboli Vieira operated efficiently the SEM for the analyses, both at UFRGS. EPMA determinations at the Microscopy and Microanalysis Laboratory of Universidade Federal de Ouro Preto were supported by the FAPEMIG-supported Microscopy and Microanalysis Network of Minas Gerais, Brazil. Field and laboratory studies were financed by Conselho Nacional do Desenvolvimento Científico e Tecnológico (CNPq) of Brazil — project Universal No. 403556/2021-0 granted to Léo A. Hartmann.

ARTICLE INFORMATION

Manuscript ID: 20220042. Received on: 13 JUN 2022. Approved on: 03 FEB 2023.

How to cite this article: Hartmann L.A., Johnner M., Queiroga G.N. 2023. Geochemistry of coarse quartz sinter overlying an Early Cretaceous Serra Geral quartz andesite flow, Fronteira Oeste Rift, Rio Grande do Sul, Brazil. *Brazilian Journal of Geology*, 53(1):e20220042. <https://doi.org/10.1590/2317-4889202320220042>

L.A.H.: Conceptualization, Data curation, Formal analysis, Funding acquisition, Investigation, Methodology, Project administration, Supervision, Validation, Visualization, Writing — original draft, Writing — review & editing. M.J.: Data curation, Investigation, Methodology, Writing — review & editing. G.N.Q.: Data curation, Investigation, Methodology, Writing — review & editing.

Competing interest: the authors declare no competing interests.

REFERENCES

- Bertolini G., Hartley A.J., Marques J.C., Healy D., Frantz J.C. 2021. The effects of basaltic lava flows on the petrophysical properties and diagenesis of interbedded aeolian sandstones: An example from the Cretaceous Paraná Basin, Brazil. *Petroleum Geoscience*, 27(2):petgeo2020-036. <https://doi.org/10.1144/petgeo2020-036>
- Bertolini G., Marques J.C., Hartley A.J., Da-Rosa A.A.S., Scherer C.M.S., Basei M.A.S., Frantz J.C. 2020. Controls on Early Cretaceous desert sediment provenance in south-west Gondwana, Botucatu Formation (Brazil and Uruguay). *Sedimentology*, 67(5):2672-2690. <https://doi.org/10.1111/sed.12715>
- Bossi J., Caggiano W. 1974. Contribuição a la geología de los yacimientos de amatista del Departamento de Artigas. In: Congresso Brasileiro de Geologia, 28., 1974, Porto Alegre. *Annals...* SBG, p. 301-317.
- Cerva-Alves T., Hartmann L.A., Queiroga G.N., Lana C., Castro M.P., Maciel L.A.C., Remus M.V.D. 2021. Metamorphic evolution of the juvenile Serrinha forearc basin in the southern Brasiliano Orogen. *Precambrian Research*, 365:106394. <https://doi.org/10.1016/j.precamres.2021.106394>
- Churchill D.M., Manga M., Hurwitz S., Peek S., Damby D.E., Conrey R., Wood J.R., McCleskey R.B., Keller W.E., Hosseini B., Hungerford J.D.G. 2021. The structure and volume of large geysers in Yellowstone National Park, USA and the mineralogy and chemistry of their silica sinter deposits. *Journal of Volcanology and Geothermal Research*, 419:107391. <https://doi.org/10.1016/j.jvolgeores.2021.107391>
- Clement A.M., Tackett L.S., Ritterbush K.A., Ibarra Y. 2020. Formation and stratigraphic facies distribution of early Jurassic iron oolite deposits from west central Nevada, USA. *Sedimentary Geology*, 395:105537. <https://doi.org/10.1016/j.sedgeo.2019.105537>
- Deer W.A., Howie R.A., Zussman J. 1966. *An Introduction to the Rock-Forming Minerals*. Addison-Wesley: Longman.
- Duarte L.C., Hartmann L.A., Vasconcellos M.A.Z., Medeiros J.T.N., Theye T. 2009. Epigenetic formation of amethyst-bearing geodes from Los Catalanes gemological district, Artigas, Uruguay, southern Paraná Magmatic Province. *Journal of Volcanology and Geothermal Research*, 184(3-4):427-436. <https://doi.org/10.1016/j.jvolgeores.2009.05.019>
- Duarte S.K., Hartmann L.A., Baggio S.B. 2020. Fluidized sand effusion over successive basalt flows of the northwestern Paraná volcanic province. *Journal of South American Earth Sciences*, 99:102505. <https://doi.org/10.1016/j.jsames.2020.102505>
- Fenner E.R., Bruesecke M.E., Shaulis B.J. 2022. Archetypal Au-bearing silica sinter from the Miocene Milestone deposit, Idaho, USA. *Mineralium Deposita*, 58, 223-241. <https://doi.org/10.1007/s00126-022-01117-z>
- Gilg H.A., Morteani G., Kostitsyn Y., Preinfalk C., Gatter I., Strieder A.J. 2003. Genesis of amethyst geodes in basaltic rocks of the Serra Geral Formation (Ametista do Sul, Rio Grande do Sul, Brazil): a fluid inclusion, REE, oxygen, carbon and Sr isotope study on basalt, quartz, and calcite. *Mineralium Deposita*, 38(8):1009-1025. <https://doi.org/10.1007/s00126-002-0310-7>

- Gomes A.S., Vasconcelos P.M. 2021. Geochronology of the Paraná-Etendeka large igneous province. *Earth-Science Reviews*, **220**:103716. <https://doi.org/10.1016/j.earscirev.2021.103716>
- Gomes M.E.B. 1996. *Mecanismos de resfriamento, estruturação e processos pós-magmáticos em basaltos da Bacia do Paraná – Região de Frederico Westphalen (RS)*. Doctoral Thesis, Instituto de Geociências, Universidade Federal do Rio Grande do Sul.
- Hartmann L.A., Baggio S.B., Brückmann M.P., Knijnik D.B., Lana C., Massonne H.J., Opitz J., Pinto V.M., Sato K., Tassinari C.C.G., Arena K.R. 2019. U-Pb geochronology of Paraná volcanics combined with trace element geochemistry of the zircon crystals and zircon Hf isotope data. *Journal of South American Earth Sciences*, **89**:219-226. <https://doi.org/10.1016/j.jsames.2018.11.026>
- Hartmann L.A., Cerva-Alves T. 2021. Resurfaced paleodunes from the Botucatu erg amid Cretaceous Paraná volcanics. *Geomorphology*, **383**:107702. <https://doi.org/10.1016/j.geomorph.2021.107702>
- Hartmann L.A., Duarte L.C., Massonne H.J., Michelin C., Rosenstengel L.M., Bergmann M., Theye T., Pertille J., Arena K.R., Duarte S.K., Pinto V.M., Barboza E.G., Rosa M.L.C.C., Wildner W. 2012. Sequential opening and filling of cavities forming vesicles, amygdalae and giant amethyst geodes in lavas from the southern Paraná volcanic province, Brazil and Uruguay. *International Geology Review*, **54**(1):1-14. <https://doi.org/10.1080/00206814.2010.496253>
- Hartmann L.A., Pertille J., Bicca M.M., Santos C.B. 2022a. Hydrothermal bowls in the giant Cretaceous Botucatu paleoerg. *Brazilian Journal of Geology*, **52**(1):e20210058. <https://doi.org/10.1590/2317-4889202220210058>
- Hartmann L.A., Pertille J., Bicca M., Santos C.B., Johner M., Cerva-Alves T. 2022b. Silicification, fracturing and steam venting of Botucatu paleodunes in the Early Cretaceous. *Journal of South American Earth Sciences*, **118**:103924.
- Hartmann L.A., Pertille J., Cerva-Alves T., Duarte S.K. 2021. Paraná quartz andesite rings and arcs formed by distal imprint of dune design from the Botucatu paleoerg. *Journal of South American Earth Sciences*, **112**(Part 2):103612. <https://doi.org/10.1016/j.jsames.2021.103612>
- Hartmann L.A., Wildner W., Duarte L.C., Duarte S.K., Pertille J., Arena K.R., Martins L.C., Dias N.L. 2010. Geochemical and scintillometric characterization and correlation of amethyst geode-bearing Paraná lavas from the Quaraí and Los Catalanes districts, Brazil and Uruguay. *Geological Magazine*, **147**(6):954-970. <https://doi.org/10.1017/S0016756810000592>
- Hirata R., Foster S. 2021. The Guarani Aquifer System – from regional reserves to local use. *Quarterly Journal of Engineering Geology and Hydrogeology*, **54**(1):qjehg2020-091. <https://doi.org/10.1144/qjehg2020-091>
- International Mineralogical Association (IMA). 2022. *Classification of minerals*. IMA. Available at: <http://www.webmineral.com/>. Accessed on: Dec 5, 2022.
- Jones B. 2021. Siliceous sinters in thermal spring systems: Review of their mineralogy, diagenesis, and fabrics. *Sedimentary Geology*, **413**:105820. <https://doi.org/10.1016/j.sedgeo.2020.105820>
- Juchem P.L. 1999. *Mineralogia, geologia e gênese dos depósitos de ametista da região do Alto Uruguai, Rio Grande do Sul*. 224 p. Tese de Doutorado, Programa de Pós-Graduação em Geociências, Instituto de Geociências, Universidade de São Paulo, São Paulo.
- Kharaka Y.K., Sorey M.L., Thordsen J.J. 2000. Large-scale hydrothermal fluid discharges in the Norris–Mammoth corridor, Yellowstone National Park, USA. *Journal of Geochemical Exploration*, **69-70**:201-205. [https://doi.org/10.1016/S0375-6742\(00\)00025-X](https://doi.org/10.1016/S0375-6742(00)00025-X)
- Marcoux E., Le Berre P., Cocherie A. 2004. The Meillers Autunian hydrothermal chalcidony: first evidence of a 295 Ma auriferous epithermal sinter in the French Massif Central. *Ore Geology Reviews*, **25**(1-2):69-87. <https://doi.org/10.1016/j.oregeorev.2003.10.001>
- Rivas-Sanchez M.L., Alva-Valdivia L.M., Arenas-Alatorre J., Urrutia-Fucugauchi J., Ruiz-Sandoval M., Ramos-Molina M.A. 2006. Berthierine and chamosite hydrothermal: genetic guides in the Peña Colorada magnetite-bearing ore deposit, Mexico. *Earth Planets Space*, **58**:1389-1400. <https://doi.org/10.1186/BF03352635>
- Santos J.O.S., Hartmann L.A. 2021. Chemical classification of common volcanic rocks based on degree of silica saturation and CaO/K₂O ratio. *Annals of the Brazilian Academy of Sciences*, **93**(3):e20201202. <https://doi.org/10.1590/0001-3765202120201202>
- Silva M.A.S., Favilla C.A.C., Wildner W., Ramgrab G.E., Lopes R.C., Sachs L.L.B., Silva V.A., Batista I.H. 2004. Folha SH.21-Uruguaiana. In: Schobbenhaus C., Gonçalves J.H., Santos J.O.S., Abram M.B., Leão Neto R., Matos G.M.M., Vidotti R.M., Ramos M.A.B., Jesus J.D.A. (Eds.), *Carta Geológica do Brasil ao Milionésimo*. Sistema de Informações Geográficas. Programa Geologia do Brasil. Brasília: CPRM. CD-ROM.
- Tan C., Fowler A., Tutor A., Seyfried Jr. W.E. 2020. Heat and mass transport in sublacustrine vents in Yellowstone Lake, Wyoming: In-situ chemical and temperature data documenting a dynamic hydrothermal system. *Journal of Volcanology and Geothermal Research*, **405**:107043. <https://doi.org/10.1016/j.jvolgeores.2020.107043>
- Teixeira C.A.S., Sawakuchi A.O., Bello R.M.S., Nomura S.F., Bertassoli D.J., Chamani M.A.C. 2018. Fluid inclusions in calcite filled opening fractures of the Serra Alta Formation reveal paleotemperatures and composition of diagenetic fluids percolating Permian shales of the Paraná Basin. *Journal of South American Earth Sciences*, **84**:242-254. <https://doi.org/10.1016/j.jsames.2018.04.004>
- Whitney D.L., Evans B.W. 2010. Abbreviations for names of rock-forming minerals. *American Mineralogist*, **95**(1):185-187. <https://doi.org/10.2138/am.2010.3371>
- Zalán P.V., Wolff S., Astolfi M.A.M., Vieira I.S., Conceição J.C.J., Appi V.T., Neto E.V.S., Cerqueira J.R., Marques A. 1991. The Paraná basin, Brazil. In: Leighton M.W., Kolata D.R., Oltz D.F., Eidel, J.J. (Eds.), *Interior Cratonic Basins. American Association of Petroleum Geologists Memoir*, **51**:681-708.
- Zane A., Weiss Z. 1998. A procedure for classifying rock-forming chlorites based on microprobe data. *Rendiconti Lincei Science Fisiche e Naturali*, **9**:51-56. <https://doi.org/10.1007/BF02904455>